JJEE

Volume 12 | Number 3 | September 2026 | Pages 416-428

Jordan Journal of Electrical Engineering

ISSN (print): 2409-9600, ISSN (online): 2409-9619

Homepage: jjee.ttu.edu.jo

Poly (3, 4-ethylenedioxythiophene) - Manganese Oxide Solid-State Supercapacitors: Synthetic Route Adjustment for Enhanced Electrical Energy Storage Performance

Amr M. Obeidat[1*]

[1] Department of Electrical Engineering, Faculty of Engineering, The Hashemite University, P.O Box 330127, Zarqa 13133, Jordan

E-mail: amrobeidat@hu.edu.jo

Received: Jan 23, 2026 *Revised: Mar 07, 2026* *Accepted: Apr 22, 2026* *Available online: Aug 15, 2026*

***Abstract*—** Poly (3, 4-ethylenedioxythiophene) (PEDOT)– Manganese Oxide (MnO_2) composite electrodes were made to assemble a symmetrical solid-state supercapacitor. The electrode was prepared by different synthetic routes; the first one was obtained by dipping a pulsed polymerized PEDOT film inside a solution mixture of potassium permanganate $KMnO_4$ and manganese sulfate $MnSO_4$, and the second one was obtained by dipping the PEDOT film inside $KMnO_4$, which resulted in a thinner MnO_2 layer, and thus better results. The presence of MnO_2 was confirmed by the symmetrical stretching vibration of the MnO_6 groups and the peak corresponding to Lithium Birenessite, with reference to the relevant literature. The optimum MnO_2 thickness was reached by soaking the PEDOT electrode in the MnO_2 solution for 10 minutes, reaching a 40°C temperature, which corresponded to the thinnest MnO_2 layer. The optimum PEDOT thickness was achieved by adjusting the number of cycles to 20K, resulting in the thickest PEDOT film with the highest conductivity. The supercapacitor exhibited a maximum capacitance of 122.08 mF cm^{-2} at 10 mVs^{-1}. The ultimate specific energy and power values were 26.19 Wh kg^{-1} and 6.09 kW kg^{-1}. The supercapacitor device showed a stable electrochemical behavior when subjected to a charge-discharge life test of 1000 consecutive cycles with an average Coulomb efficiency of 94.6%.

***Keywords*—** PEDOT; Manganese Oxide; Electrochemical Co-deposition; Electrochemical energy storage; Solid-state Supercapacitors.

1. INTRODUCTION

Supercapacitors are thoroughly investigated because of their distinct features of high power density, intermediate energy density, rapid charge-discharge rates, and other characteristics [1,2]. These remarkable properties make them an integral part in many modern applications such as flexible and portable electronic devices [3,4]. However, a major challenge in this context is their relatively low energy densities, and therefore, numerous research efforts have been dedicated to boosting their specific energy. The energy stored in a supercapacitor can be enhanced by either increasing the capacitance or the potential range of the active electrode or both. This can be accomplished through a variety of approaches such as manipulating the electrode's structure, using composite materials, or choosing the suitable type of electrolyte. Although, the supercapacitors made with conventional aqueous electrolytes achieved remarkable energy storage functionalities, their performance has been restricted by the potential window and other practical limitations such as the bulky size and the corrosion problems. On the other hand, solid-state supercapacitors with ionic liquid electrolytes offer a compact, safe, and efficient platform that can ultimately boost the specific energy of the device.

* Corresponding author

DOI: https://doi.org/10.5455/jjee.204-1769148726

Pseudo-capacitive electrodes generally include conducting polymers and transition metal oxides. Among the different types of metal oxides, Ruthenium Oxide (RuO_2) displays the utmost pseudo-capacitive behavior, however, its highly performing character is restricted by its high cost [5-9]. Manganese Oxide (MnO_2) is a good replacement due to its high theoretical capacitance (1370 F g^{-1}), low cost, and environmental benignity [10-16]. On the other hand, MnO_2 has a dense morphology and poor electrical conductivity (10^{-5} – 10^{-6} S cm^{-1}) [17-19], therefore it has to be combined with another material to take the advantage of its properties. One possible approach is to combine it with conducting polymers such as polyaniline, polypyrrole, and PEDOT. Among them, PEDOT shows excellent electrical conductivity, good electrochemical and mechanical stability, and a wide potential window [20-22]. In this research, PEDOT-Manganese oxide electrodes were synthesized by two different mechanisms that basically involve the immersion of pulsed polymerized PEDOT in MnO_2 solution. The reason behind selecting two different manganese oxide precursor solutions is to boost the electrochemical energy storage performance of the given device by adjusting the synthesis route and controlling the various relevant parameters such as thickness and concentration. The novelty of this work lies in the fact that ionic liquid gel polymer electrolyte was used to create a flexible, compact, reliable, and solid-state platform that is more suitable for the next generation of energy storage devices, while on the other hand the majority of the work that has been done so far in this area was based on conventional aqueous electrolytes. There have been a few studies in the literature about PEDOT-MnO_2 supercapacitors. For example, PANI/PEDOT:PSS/MnO_2 has been used recently as a ternary composite electrode material for supercapacitor application [23]. In another study, MnO_2/PEDOT:PSS-reduced graphene oxide nanocomposite electrode was used to fabricate a 2.8-Volt asymmetric micro-supercapacitor [24]. However, the objective of this research is to improve upon the device functions by introducing PEDOT-MnO_2 solid-state supercapacitors that were prepared by dip coating (or soaking) of PEDOT in manganese oxide solution based on two different synthetic routes with various parameters being studied. The results of the present work are competitive and outperform the results previously mentioned in the relevant literature. To further show the significance and the competence of this work, Table 1 compares the results achieved in this work with the state-of-the art PEDOT-MnO_2 supercapacitors.

Table 1. Comparison of energy storage functionalities for various PEDOT-MnO_2 supercapacitors.

Electrode Composition	Specific Capacitance	Energy/Power Density	Reference
PEDOT soaked with MnO_2	122.08 mF cm^{-2} at 10 mV s^{-1}	Energy density = 26.19 Wh kg^{-1} Power Density = 6.09 kW kg^{-1}	This work
MnO_2 nanoparticles decorated PEDOT:PSS	1.14 mF cm^{-2}	--	[25]
MnO_2/PEDOT microelectrodes	43 mF cm^{-2}	5.1 µWh cm^{-2}	[26]
PEDOT:PSS/MnO_2	87.4 F g^{-1} at 5 mV s^{-1}	--	[27]
PEDOT-MnO_2 prepared by single-step co-deposition	73.81 mF cm^{-2} at 10 mV s^{-1}	Energy density = 15.07 Wh kg^{-1} Power Density = 6.84 kW kg^{-1}	[28]

The first and major contribution of this work is to create a solid-state and compact electrochemical energy storage platform by utilizing ionic liquid gel polymer electrolyte. On the other hand, numerous work has been done so far in this area based on conventional aqueous electrolytes that have many limitations as explained earlier in the introduction.

Another contribution of this work is to offer a synthetic route adjustment approach in an effort to optimize the device functionalities for such a polymer-metal oxide system. The third contribution is to study the impact of varying thickness and concentration parameters on the capabilities of the device.

2. EXPERIMENT

2.1. Electrode Synthesis

2.1.1. Electrode synthesis by dip coating in a solution mixture of $KMnO_4$ and $MnSO_4$

The PEDOT film in this case was prepared by pulsed electro-polymerization on graphite substrates in 0.1 M lithium perchlorate ($LiClO_4$) with 0.01 M EDOT monomer in acetonitrile. Unipolar sequential anodic current pulses of current density of 4 mA cm^{-2} of 10 ms on period and 100 ms off period were applied to form the PEDOT film. The MnO_2 solution was prepared by mixing potassium permanganate ($KMnO_4$) and manganese sulfate ($MnSO_4$) using different molar concentrations for both materials. $KMnO_4$ concentrations of 0.12, 0.16, and 0.25 M and $MnSO_4$ concentrations of 0.1, 0.13, and 0.2 M were used. Solutions were prepared by dissolving $KMnO_4$ and $MnSO_4$ separately in deionized water by magnetic stirring for 10 minutes at room temperature. Both solutions were then mixed together by gradually adding $MnSO_4$ solution to $KMnO_4$ solution to form the complete liquid mixture of MnO_2.

The composite film was prepared by simple immersion of PEDOT in this solution that was heated for a specific amount of time (details on this process are given later in the paper). After reaching the desired temperature of the solution, the sample was removed and naturally dried overnight.

2.1.2. Electrode synthesis by simple immersion in $KMnO_4$ solution

First of all, the PEDOT electrode was prepared by the electro-polymerization process based on optimized 20 K-cycle thickness. The second step was to prepare the $KMnO_4$ solution by dissolution of 0.1 M $KMnO_4$ powder in 100 ml of DI water by mechanical stirring for approximately 10 minutes. The third step was to heat the $KMnO_4$ solution for about half an hour until temperature reached 40°C.

The fourth step was to immerse the PEDOT film inside the $KMnO_4$ solution for about 10-15 minutes, and then take it out and heat it for 5 minutes inside an oven under a constant temperature of 90°C. The final stage was to allow the composite electrode to dry naturally overnight before using it to assemble the supercapacitor.

2.2. Preparation of Electrolyte and Supercapacitor Cell

First of all, the host polymer PVdF-HFP was dissolved in acetone and then doped with 0.1 M $LiClO_4$. Afterwards, the ionic liquid $BMIMBF_4$ was added to the polymer solution under a weight ratio of 80:20, and it was wriggled by the influence of a magnetic capsule for approximately 10 h.

The resultant electrolyte solution was spread on the active area of both electrodes and the acetone was allowed to evaporate naturally at room temperature. The electrodes were stacked and clipped together with a light force and the resultant supercapacitor device was left overnight before recording the measurements.

2.3. Electrochemical Measurements

The cyclic voltammetry and charge-discharge measurements were taken using the Solartron Electrochemical Interface (Model 1287), and the EIS measurement was taken using the gain-phase impedance analyzer (Model: 1260). The Raman spectra were generated using the DXR Raman microscope with 532- nm excitation laser.

3. RESULTS AND DISCUSSION

Before proceeding with the results, the supercapacitor that was prepared by immersing PEDOT inside a solution mixture of $KMnO_4$ and $MnSO_4$ was designated as SD1, and the supercapacitor that was prepared by simple immersion of PEDOT in $KMnO_4$ solution was designated as SD2.

3.1. Assessment of Electrochemical Performance for SD1

The basic electrochemical measurements were taken out and depicted in Fig. 1.

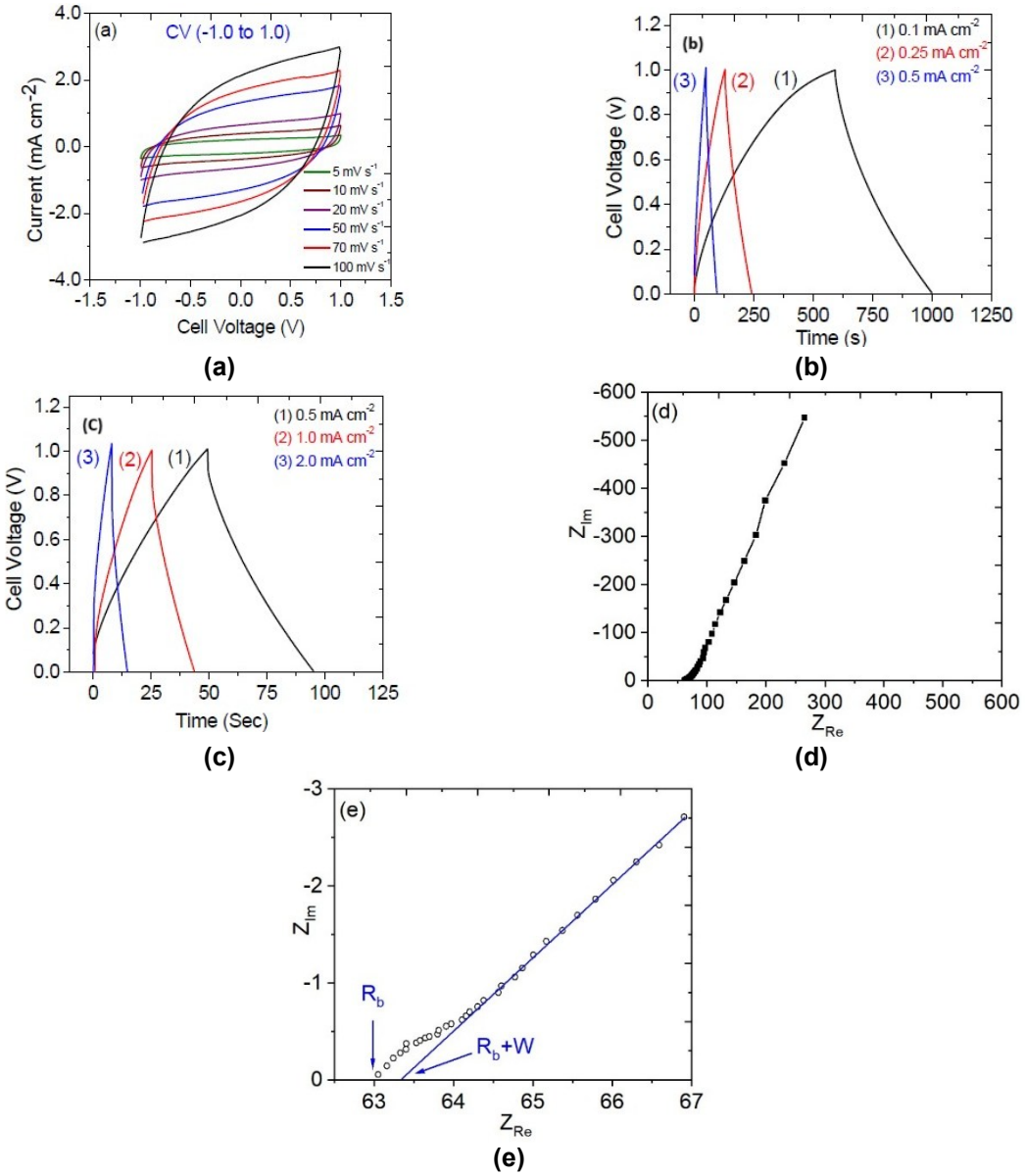

Fig. 1. Basic electrochemical measurements for SD1, including a) CV; b) and c) CD conducted at a diverse range of current densities; d) EIS; and e) high-frequency region in the EIS spectrum.

The CV measurement was done in the potential domain (-1 to 1) V at a variety of scan rates ranging from 5 up to 100 mV s^{-1} as seen in Fig. 1a. The maximum capacitance of 69.95 mF cm^{-2} was noted at 5 mV s^{-1}. The pseudo-capacitive features are dominant in SD1 as can be inferred from the shape of the curves. The CD measurement was performed at a variety of current densities starting from 0.1 mA cm^{-2} up to 2 mA cm^{-2} (as seen in Fig. 1b & 1c), showing typical pseudo-capacitive charge storage processes with a resistance of 47.9 Ω cm^2. The impedance spectroscopy measurement was also conducted and a Nyquist plot was generated showing the real and imaginary components of the impedance (Fig. 1d). The high-frequency region in the EIS spectrum is used to evaluate the resistances of a supercapacitor device, and is shown in Fig. 1e. The Warburg resistance was noted as 0.293 Ω cm^2 indicating low diffusion kinetics and good ion propagation at the interface between the electrode and the electrolyte. The bulk resistance was found to be 63.05 Ω cm^2.

3.2. Life Test Measurement

The life test performance for SD1 was evaluated by repeatedly charging and discharging for 1000 cycles at 0.25 mA cm^{-2}. Figure 2a shows the change in capacitance values versus cycle number. It is interesting to note that the capacitance marginally degrades from 26.51 mF cm^{-2} to 20.48 mF cm^{-2} over the first 550 cycles. However, after the 550th cycle, the capacitance increases from 20.48 mF cm^{-2} to 25.01 mF cm^{-2} over the second half of the test. Figure 2b shows the change of the Coulombic efficiency versus the cycle number. The Coulombic efficiency gradually increases from 92.06% to 97.15% over the first 400 cycles, and then remains stable up to 1000 cycles.

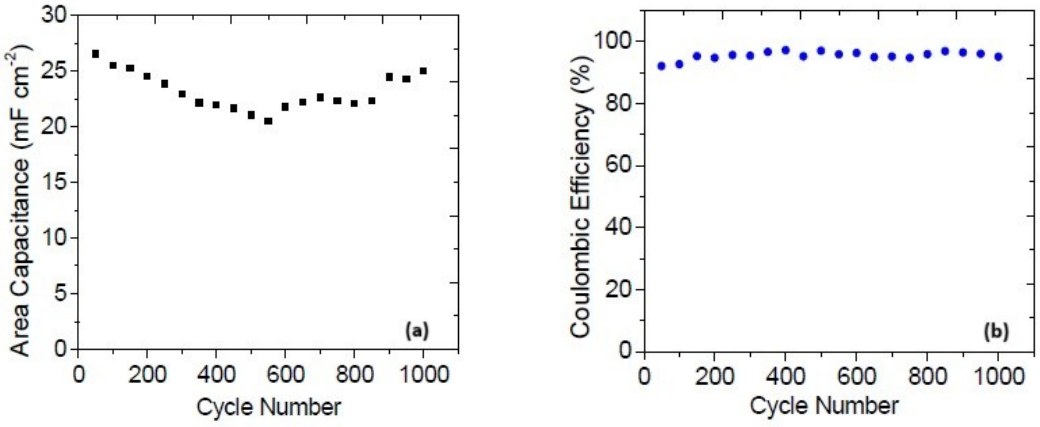

Fig. 2. Change in a) capacitance; b) Coulombic efficiency vs. the cycle number for SD1.

3.3. Raman Spectroscopy

The electrode's composition was verified by Raman spectroscopy, as shown in Fig. 3. The presence of PEDOT was authenticated by the crests 570, 983, 1112, 1238, and 1433 cm^{-1} [29]. The presence of MnO_2 was confirmed by the crests located at 435 cm^{-1} and 630 cm^{-1}. The crest noticed at 630 cm^{-1} is approximately near to 642 cm^{-1} mentioned in [30] and 640 cm^{-1} mentioned in [31] that was attributed to the symmetric stretching vibration (Mn-O) of the MnO_6 groups. The crest noticed at 435 cm^{-1} is close to 410 cm^{-1} documented in [32] that was identified as Lithium Birnessite.

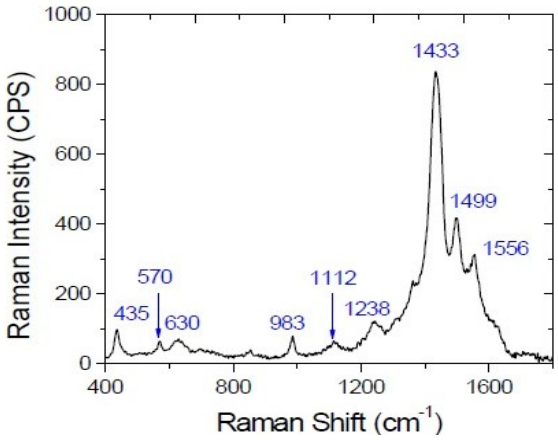

Fig. 3. Raman signature of the PEDOT-Manganese Oxide electrode.

4. EFFECT OF MnO_2 CONCENTRATION

One of the main factors that directly affect the morphology of MnO_2 is the concentration of the deposited MnO_2 primarily due to rapid oxidation and growth of MnO_2 in the dipping solution consisting of $MnSO_4$ and $KMnO_4$. To investigate that impact on the properties of the supercapacitor, three symmetrical PEDOT-MnO_2 supercapacitors were produced with various concentrations of $MnSO_4$ and $KMnO_4$ as follows:

- Cell 1 was prepared with 0.12 M $KMnO_4$ and 0.1 M $MnSO_4$
- Cell 2 was prepared with 0.16 M $KMnO_4$ and 0.13 M $MnSO_4$
- Cell 3 was prepared with 0.25 M $KMnO_4$ and 0.2 M $MnSO_4$.

Figure 4 shows the CV curves of the three cells at 20 mV s^{-1}. Although the shape of the CV curves shows consistent pseudo-capacitive character, it is clear that the area of the CV loop is greatly dependent upon the MnO_2 concentration that directly affects its morphology. Cell 1 displayed the largest CV loop area and the largest working electrode current that created a capacitance of 60.69 mF cm^{-2}. Cell 2 displayed an intermediate current density with a capacitance of 49.84 mF cm^{-2}. Cell 3 displayed the smallest CV capacitance of 31.15 mF cm^{-2}. Based on this discussion, ascending capacitance values are noticed for less concentrations of $KMnO_4$ and $MnSO_4$. Considering CD analysis, Cells 1 and 2 produced capacitances of 25.62 and 25.01 mF cm^{-2}, respectively, and resistance values of 56.2 and 48.6 Ω cm^2, respectively. However, Cell 3 produced the lowest capacitance of 12.13 mF cm^{-2} and much higher resistance of 178 Ω cm^2. EIS shows that Cells 1 and 2 produced capacitances of 34.09 mF cm^{-2} and 29.13 mF cm^{-2}, respectively, and bulk resistances of 76.53 and 62.91 Ω cm^2, respectively. However, Cell 3 displayed the lowest capacitance of 17.54 mF cm^{-2} and the highest resistance of 198.90 Ω cm^2, which means that the increasing MnO_2 concentration leads to a higher bulk resistance. From the preceding discussion, it is noted that the morphology of the MnO_2 layer can be affected and controlled based on $MnSO_4$ and $KMnO_4$ concentrations. Less MnO_2 concentrations produce better electrode morphology and ion propagation at the electrode-electrolyte interface. Table 2 compares capacitance values as functions of molar concentrations.

Table 2. Effect of $KMnO_4$ and $MnSO_4$ molar concentrations on capacitance.

$KMnO_4$ [M]	$MnSO_4$ [M]	CV (mF cm^{-2}) at 20 mV s^{-1}	CD (mF cm^{-2}) at 0.5 mA cm^{-2}	EIS (mF cm^{-2})
0.12	0.1	60.69	25.62	34.09
0.16	0.13	49.84	25.01	29.13
0.25	0.2	31.15	12.13	17.54

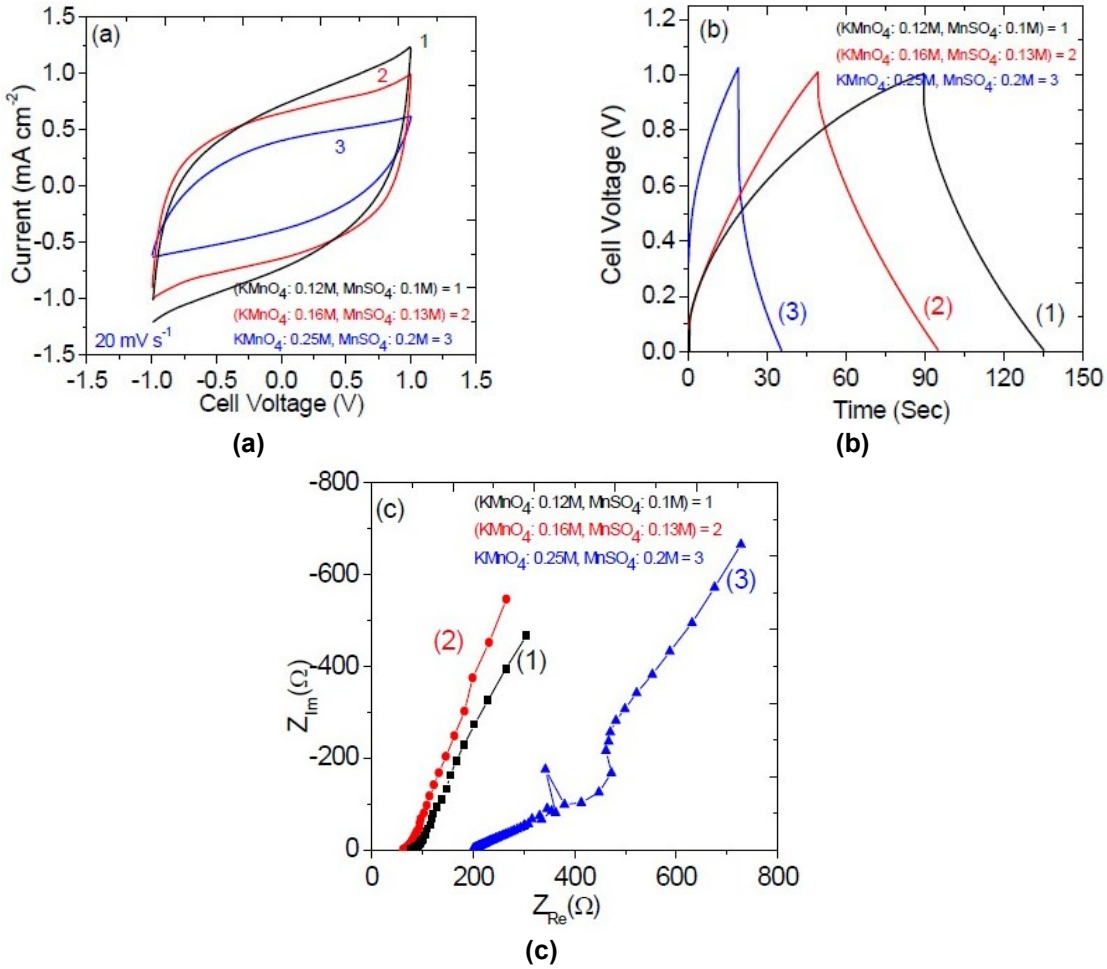

Fig. 4. Impact of $KMnO_4$ and $MnSO_4$ concentrations on SD1 performance.

5. EFFECT OF MnO_2 THICKNESS

The effect of MnO_2 thickness was studied by fabricating three different supercapacitor devices. The first electrode was synthesized by dipping PEDOT in the solution for 10 minutes until the solution's temperature reached 40°C. The second electrode was prepared by dipping PEDOT inside MnO_2 solution for 25 minutes until the temperature reached 70°C. And the third electrode was prepared by dipping PEDOT inside MnO_2 solution for 1 hour until the temperature reached 81°C. The three supercapacitor cells were designated based on electrode synthesis conditions as follows:

- Cell 1: 40°C, 10 min
- Cell 2: 70°C, 25 min
- Cell 3: 81°C, 1h.

It is noteworthy to mention that, according to the experimental observations, MnO_2 thickness directly depends on the soaking time and solution temperature simultaneously. Longer soaking time and higher temperatures increase the thickness of the MnO_2 layer and thus the conductivity decreases because MnO_2 has inherent low electrical conductivity.

Figure 5 demonstrates the effect of MnO_2 thickness on the device functions in terms of CV and EIS. Considering the CV measurement at 20 mV s^{-1}, the capacitances 31.15 mF cm^{-2}, 6.78 mF cm^{-2}, and 8.26 mF cm^{-2} were obtained for Cells 1, 2, and 3, respectively. The EIS measurement for Cell 1 resulted in the highest capacitance of 17.54 mF cm^{-2} and the lowest resistance of 198.89 Ω cm^2. Cells 2 and 3 produced capacitances of 3.34 and 12.98 mF cm^{-2},

respectively, and bulk resistances of 1037.2 and 1604.6 Ω cm^2 were noted, respectively. Table 3 summarizes these results.

Table 3. Effect of MnO_2 thickness (controlled by temperature and soaking time) on capacitance values.

Soaking Time	Temperature	CV [mF cm^{-2}]	EIS [mF cm^{-2}]	R_b [Ω cm^2]
10 min	40°C	31.147	17.54	198.89
25 min	70°C	6.78	3.34	1037.2
1 hour	81°C	8.26	12.98	1604.6

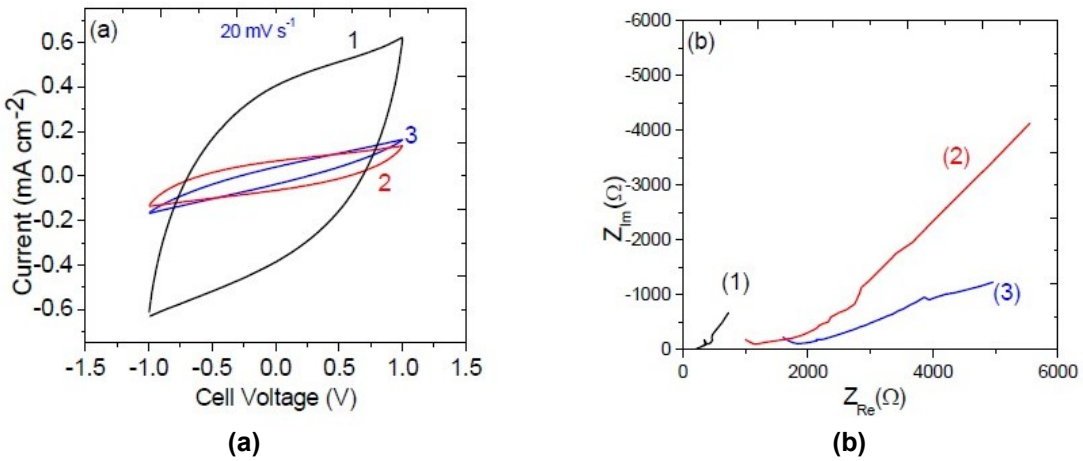

(a) (b)

Fig. 5. Effect of MnO_2 thickness on SD1 performance.

6. EFFECT OF PEDOT THICKNESS

The effect of PEDOT thickness on SD1 performance was also investigated by synthesizing various PEDOT electrodes of different thicknesses including 20K, 12K, and 9K number of cycles during the pulsed current electro-polymerization process. It is scientifically established that low electrical conductivity is one of the inherent properties of MnO_2. Therefore, it is vital to compensate for this disadvantage by adding PEDOT with high conductivity. Figure 6 demonstrates the impact of PEDOT thickness on the capacitive attributes of SD 1. Considering the CV data, the maximum capacitance of 31.15 mF cm^{-2} was achieved at 20 mV s^{-1} for 20K number of cycles corresponding to the highest PEDOT thickness. A middle capacitance of 19.65 mF cm^{-2} was observed for 12K cycles, and the lowest CV capacitance value of 12.482 mF cm^{-2} was observed for the supercapacitor with the lowest PEDOT thickness adjusted with 9K cycles. Similarly, the remaining outcomes confirm the preceding argument, as summarized in Table 4.

Table 4. Effect of PEDOT thickness on SD 1 performance.

Cycle Number	CV [mF cm^{-2}] at 20 mV s^{-1}	CD [mF cm^{-2}] at 0.1 mA cm^{-2}	EIS [mF cm^{-2}]
20 K	31.15	27.78	17.54
12 K	19.65	12.96	10.51
9 K	12.482	4.54	6.31

7. ASSESSMENT OF ELECTROCHEMICAL PERFORMANCE FOR SD2

As demonstrated earlier in this paper, the supercapacitor device SD2 was prepared by simple immersion of PEDOT inside $KMnO_4$ solution, and the details of electrode synthesis were provided in the experimental section. Interestingly, this synthetic route produced significantly

improved results due to better pseudo-capacitive activity as it is explained in the upcoming discussion.

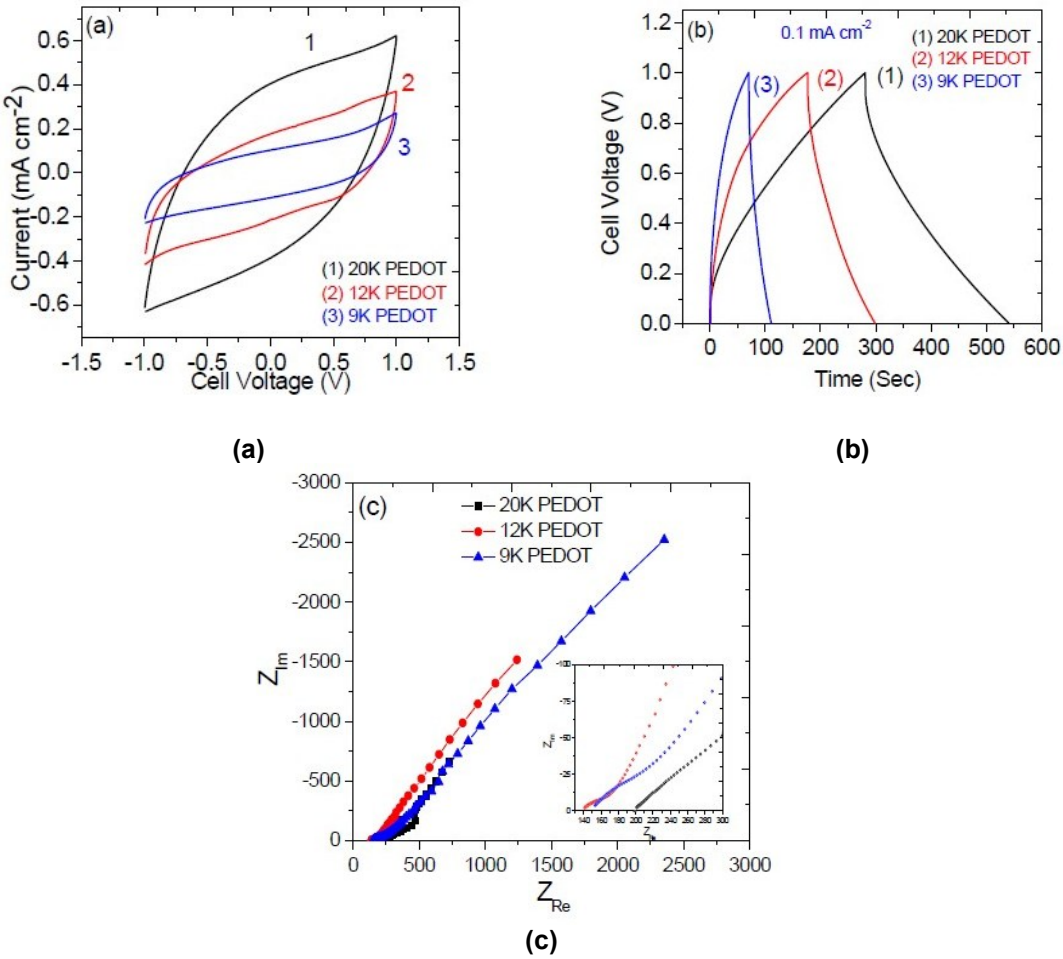

Fig. 6. Effect of PEDOT thickness on SD1 Performance.

7.1. CV and Specific Energy/ Power Studies

Using this synthesis technique resulted in the deposition of a very thin MnO_2 layer on the surface of PEDOT achieving a capacitance of 122.08 mF cm^{-2} at 10 mV s^{-1}. Specific power and energy values were extracted from the charge-discharge test and they were plotted in Fig. 7b, indicating enhanced energy storage processes. The utmost values for the y-axis and x-axis were proved to be 26.19 Wh kg^{-1}, and 6.09 kW kg^{-1}, respectively. The specific energy/power analysis was performed based on a total electrode mass of 1.6 mg cm^{-2}.

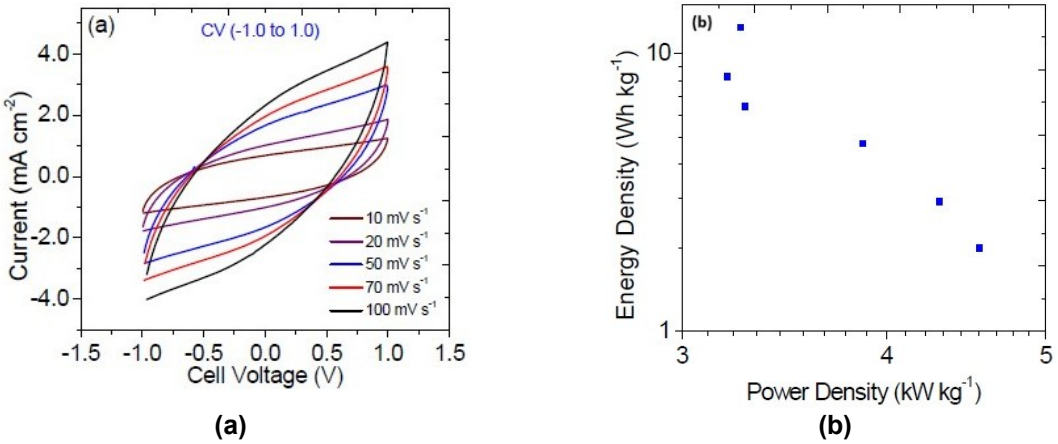

Fig. 7. (a) CV; b) ragone plot for the SD 2 device.

7.2. CD and EIS Functionalities for SD 2

The charge/discharge and impedance profiles were generated to further evaluate the SD 2 device functionalities, as depicted in Fig. 8. The CD curves for SD 2 exhibit linear and symmetrical features with an ESR value of 39.6 Ω cm^2 at 0.25 mA cm^{-2}. On the other hand, the ESR value for SD 1 was noted to be 49.2 Ω cm^2 at the same current density, meaning that SD 2 is more efficient in terms of energy storage as compared to SD 1. Furthermore, a Nyquist plot was generated for SD 2 with a bulk resistance of 27.46 Ω cm^2 which is significantly less than SD 1 that displayed a bulk resistance of 63.05 Ω cm^2. To conclude, the SD 2 device is a highly performing device and showed a better and more efficient electrochemical activity by all means when compared to SD 1.

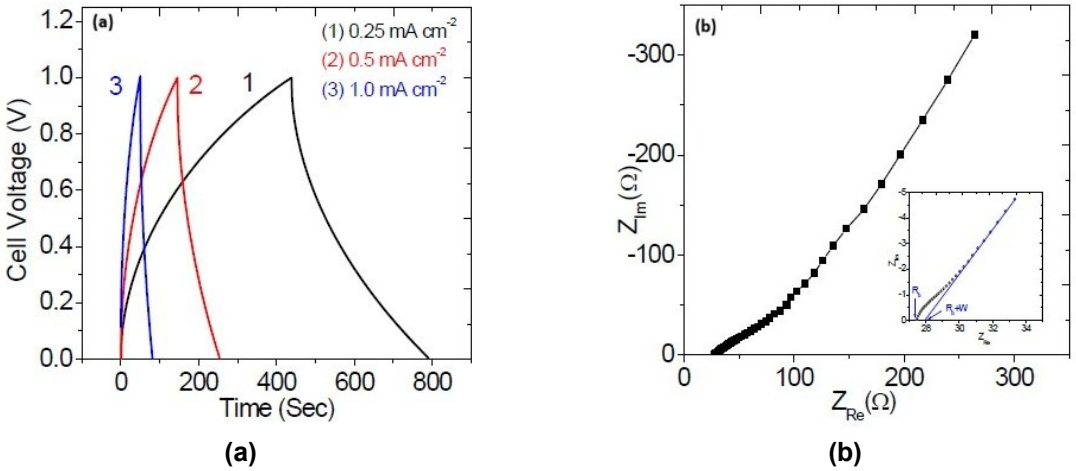

Fig. 8. a) CD; b) EIS data for the SD 2 device.

8. CONCLUSIONS

The main outcome of this study is that the PEDOT-MnO_2 synthesis procedure has a great impact on the supercapacitor device qualities. It was noted that depositing a thin layer of MnO_2 on PEDOT surface yields better results – a fact that was confirmed by comparing the results of SD1 and SD2. This study went into further details including the effect of MnO_2 concentration, MnO_2 thickness, and PEDOT thickness on SD1 performance. The optimum MnO_2 concentration was achieved with $KMnO_4$: 0.12 M and $MnSO_4$: 0.1 M. The MnO_2 thickness was controlled by soaking time, and obviously longer soaking time resulted in thicker MnO_2 layers and less conductivities, and consequently less capacitance values. The thickness of the PEDOT layer was adjusted by the number of electro-polymerization cycles. Increasing the number of cycles leads to higher PEDOT thickness with higher electrical conductivities and better electrochemical qualities.

Acknowledgements: The author acknowledges Dr. Alok C. Rastogi for his insightful guidance and unfailing support. The author also acknowledges the Center for Autonomous Solar Power (CASP) at Binghamton University, the State University of New York.

REFERENCES

[1] H. Lee, S. Kim, J. Jin, B. Chung, "PEDOT-MnO_2/rV_2O_5@graphene nanocomposite electrode-based stretchable micro-supercapacitor array with T-joint-cut kirigami structure", *Journal of Energy Storage*, vol. 118, p. 116285, 2025, doi: 10.1016/j.est.2025.116285.

[2] A. Akbar et al., "Integrated MnO_2/PEDOT composite on carbon cloth for advanced electrochemical energy storage asymmetric supercapacitors", *Journal of Power Sources*, vol. 579, p. 233181, 2023, doi: 10.1016/j.jpowsour.2023.233181.

[3] T. Nguyen, B. Soram, D. Tran, N. Kim, J. Lee, "Enhanced electrochromic capacity performances of hierarchical MnO_2 polyaniline/PEDOT:PSS/Ag@Ni nanowires cathode for flexible and rechargeable electrochromic Zn-Ion battery", *Chemical Engineering Journal*, vol. 452, p. 139555, 2023, doi: 10.1016/j.cej.2022.139555.

[4] Q. He, J. Ye, Z. Peng, Y. Guo, L. Tan, Y. Chen, "Electrodeposition of poly(3,4-ethylenedioxythiophene) coated manganese dioxide nanospheres for flexible asymmetric planar supercapacitor with superior energy density", *Journal of Power Sources*, vol. 506, p. 230176, 2021, doi: 10.1016/j.jpowsour.2021.230176.

[5] N. Azman, H. Lim, M. Mamat, Y. Sulaiman, "Synergistic enhancement of ternary Poly(3,4-ethylenedioxythiophene)/Graphene oxide/manganese oxide composite as a symmetrical electrode for supercapacitors", *Energies*, vol. 11, p. 1510, 2018, doi: 10.3390/en11061510.

[6] A. Bahloul, B. Nessark, E. Briot, H. Groult, A. Mauger, K. Zaghib, C.M. Julien, "Polypyrrole-covered MnO_2 as electrode material for supercapacitor", *Journal of Power Sources*, vol. 240, pp. 267-272, 2013, doi: 10.1016/j.jpowsour.2013.04.013.

[7] E. Rios, A. Correa, F. H. Cristovan, L. Pocrifka, A. Rosario, "Poly(3,4-ethylenedioxithiophene)/MnO_2 composite electrodes for electrochemical capacitors", *Solid State Sciences*, vol. 13, pp. 1978-1983, 2011, doi: 10.1016/j.solidstatesciences.2011.08.028.

[8] Q. Cheng, J. Tang, J. Ma, H. Zhang, N. Shinya, L. Qin, "Graphene and nanostructured MnO_2 composite electrodes for supercapacitors", *Carbon*, vol. 49, pp. 2917-2925, 2011, doi: 10.1016/j.carbon.2011.02.068.

[9] H. Xia, H. Wang, M. Lai, L. Lu, "MnO_2 nanotube and nanowire arrays by electrochemical deposition for supercapacitors", *Journal of Power Sources*, vol. 195, pp. 4410-4413, 2010, doi:10.1016/j.jpowsour.2010.01.075.

[10] M. Abdah, N. Azman, S. Kulandaivalu, N. Abdul Rahman, A. Abdullah, Y. Sulaiman, "Potentiostatic deposition of poly(3, 4-ethylenedioxythiophene) and manganese oxide on porous functionalised carbon fibers as an advanced electrode for asymmetric supercapacitor", *Journal of Power Sources*, vol. 444, p. 227324, 2019, doi: 10.1016/j.jpowsour.2019.227324.

[11] Z. Wang, J. Du, M. Zhang, J. Yu, H. Liu, X. Chai, B. Yang, C. Zhu, J. Xu, "Continuous preparation of high performance flexible asymmetric supercapacitor with a very fast, low-cost, simple and scalable electrochemical co-deposition method", *Journal of Power Sources*, vol. 437, p. 226827, 2019, doi: 10.1016/j.jpowsour.2019.226827.

[12] M. Abdah, N. Azman, S. Kulandaivalu, Y. Sulaiman, "Asymmetric supercapacitor of functionalised electrospun carbon fibers/poly(3,4-ethylenedioxythiophene)/manganese oxide//activated carbon with superior electrochemical performance", *Scientific Reports*, vol. 9, p. 16782, 2019, doi: 10.1038/s41598-019-53421-w.

[13] J. Garcia-Torres, C. Crean, "Ternary composite solid-state flexible supercapacitor based on nanocarbons/manganese dioxide/PEDOT:PSS fibres", *Materials & Design*, vol. 155, pp. 194-202, 2018, doi: 10.1016/j.matdes.2018.05.070.

[14] H. Lee, S. Park, J. Park, "Preparation and characterization of PEDOT:PSS wrapped carbon nanotubes/MnO_2 composite electrodes for flexible supercapacitors", *Synthetic Metals*, vol. 228, pp. 84-90, 2017, doi: 10.1016/j.synthmet.2017.03.016.

[15] M. Moussa, G. Shi, H. Wu, Z. Zhao, N. Voelcker, D. Losic, J. Ma, "Development of flexible supercapacitors using an inexpensive graphene/PEDOT/MnO_2 sponge composite", *Materials & Design*, vol. 125, pp. 1-10, 2017, doi: 10.1016/j.matdes.2017.03.075.

[16] E.G. Tolstopjatova, S.N. Eliseeva, A.O. Nizhegorodova, V.V. Kondratiev, "Electrochemical properties of composite electrodes, prepared by spontaneous deposition of manganese oxide into Poly-3,4-ethylendioxythiophene", *Electrochimica Acta*, vol. 173, pp. 40-49, 2015, doi: 10.1016/j.electacta.2015.05.033.

[17] M. Abdah, N. Rahman, Y. Sulaiman, "Enhancement of electrochemical performance based on symmetrical poly-(3,4-ethylenedioxythiophene) coated polyvinyl alcohol/graphene oxide/manganese oxide microfiber for supercapacitor", *Electrochimica Acta*, vol. 259, pp. 466-473, 2018, doi: 10.1016/j.electacta.2017.11.005.

[18] N. Agnihotri, P. Sen, A. De, M. Mukherjee, "Hierarchically designed PEDOT encapsulated graphene-MnO_2 nanocomposite as supercapacitors", *Materials Research Bulletin*, vol. 88, pp. 218-225, 2017, doi: 10.1016/j.materresbull.2016.12.036.

[19] P. Tang, Y. Zhao, C. Xu, "Step-by-step assembled poly(3,4-ethylenedioxythiophene)/manganese dioxide composite electrodes: Tuning the structure for high electrochemical performance", *Electrochimica Acta*, vol. 89, pp. 300-309, 2013, doi: 10.1016/j.electacta.2012.11.034.

[20] X. Li, X. Deng, Q. Li, S. Huang, K. Xiao, Z. Liu, Y. Tong, "Hierarchical double-shelled poly(3,4-ethylenedioxythiophene) and MnO_2 decorated Ni nanotube arrays for durable and enhanced energy storage in supercapacitors", *Electrochimica Acta*, vol. 264, pp. 46-52, 2018, doi: 10.1016/j.electacta.2018.01.069.

[21] N. Sidhu, A. Rastogi, "Electrochemical performance of supercapacitors based on carbon nanofoam composite and microporous poly(3, 4-ethylenedioxythiophene) thin film asymmetric electrodes", *Materials Chemistry and Physics*, vol. 176, pp. 75-86, 2016, doi: 10.1016/j.matchemphys.2016.03.028.

[22] N.K. Sidhu, A.C. Rastogi, "Bifacial carbon nanofoam-fibrous PEDOT composite supercapacitor in the 3-electrode configuration for electrical energy storage", *Synthetic Metals*, vol. 219, pp. 1-10, 2016, doi: 10.1016/j.synthmet.2016.04.012.

[23] L. Meziane, N. Boudieb, M. Seiad, I. Zaoui, I. Mechairi, A. Doumaz, "Synergistic PANI/PEDOT: PSS/MnO_2 composites electrode for superior supercapacitor performance", *Colloid and Polymer Science*, vol. 304, 277-291, 2026, doi: 10.1007/s00396-025-05524-2.

[24] L. Naderi, S. Shahrokhian, F. Soavi, "Fabrication of a 2.8 V high-performance aqueous flexible fiber-shaped asymmetric micro-supercapacitor based on MnO_2/PEDOT:PSS-reduced graphene oxide nanocomposite grown on carbon fiber electrode", *Journal of Materials Chemistry A*, vol. 8, pp. 19588-19602, 2020, doi: 10.1039/D0TA06561G.

[25] G. Liu, Z. Huang, J. Xu, T. Lin, B. Zhang, P. He, "MnO_2 nanoparticles decorated PEDOT:PSS for high performance stretchable and transparent supercapacitors", *Nanomaterials*, vol. 14, p.1080, 2024, doi: 10.3390/nano14131080.

[26] M. Tahir, L. Li, L. He, Z. Xiang, Z. Ma, W. Haider, X. Liao, Y. Song, "Interdigital MnO_2/PEDOT alternating stacked microelectrodes for high-performance on-chip microsupercapacitor and humidity sensing", *Energy & Environmental Materials*, vol. 7, p. e12546, 2024, doi: 10.1002/eem2.12546.

[27] X. Li, C. Zhou, L. Shen, W. Zhou, J. Xu, C. Luo, J. Hou, R. Tan, F. Jiang, "Flexible Free-standing PEDOT:PSS/MnO_2 films as electrode material for supercapacitors", *International Journal of Electrochemical Science*, vol. 14, pp. 4632-4642, 2019, doi: 10.20964/2019.05.12.

[28] Amr M. Obeidat, "Solid-state supercapacitors based on poly (3, 4-ethylendioxythiophene) (PEDOT)-Manganese oxide (MnO_2) composite electrodes synthesized by single-step Co-deposition for electrical energy storage", *Materials Today Energy*, vol. 10, pp. 81-88, 2018, doi: 10.1016/j.mtener.2018.08.012.

[29] S. Garreau, G. Louarn, J. Buisson, G. Froyer, S. Lefrant, "In Situ Spectroelectrochemical Raman Studies of Poly(3,4-ethylenedioxythiophene) (PEDT)", *Macromolecules*, vol. 32, pp. 6807-6812, 1999, doi: 10.1021/ma9905674.

[30] N. Chodankar, D. Dubal, G. Gund, C. Lokhande, "Flexible all-solid-state MnO_2 thin films based symmetric supercapacitors", *Electrochimica Acta*, vol. 165, pp. 338-347, 2015, doi: 10.1016/j.electacta.2015.02.246.

[31] S. Yoon, K. Kim, "Effect of poly(3,4-ethylenedioxythiophene) (PEDOT) on the pseudocapacitive properties of manganese oxide (MnO_2) in the PEDOT/MnO_2/multiwall carbon nanotube (MWNT) composite", *Electrochimica Acta*, vol. 106, pp. 135-142, 2013, doi: 10.1016/j.electacta.2013.05.058.

[32] C. Julien, M. Massot, R. Baddour-Hadjean, S. Franger, S. Bach, J. Pereira-Ramos, "Raman spectra of birnessite manganese dioxides", *Solid State Ionics*, vol. 159, pp. 345-356, 2003, doi: 10.1016/S0167-2738(03)00035-3.